

LETTER

Open Access



# Hydrophobic surface for direct PEGDA micro-pattern fabrication

Anna Danielak<sup>1\*</sup>, Juhee Ko<sup>2</sup>, Aminul Islam<sup>1</sup>, David Bue Pedersen<sup>1</sup> and Jungchul Lee<sup>2</sup>

## Abstract

Photopolymerization of hydrogels films has gained interest in many biomedical and industrial fields. Hydrogel micro-patterns fabricated directly on a device are used as filtering barriers, however, due to weak mechanical properties, these parts require a stable support but deposition of hydrogel in non-polymerized state brings a risk of sinking inside the structure. These limitations can be overcome by applying a hydrophobic surface. This paper presents a novel two-step method, in which a hydrophobic surface was designed and manufactured using mask-projection vat photopolymerization additive manufacturing (VPP). Afterwards, PEGDA-based hydrogel photopolymers were deposited on the surface and a micro-scale patterns were cured. The parts were subjected to water immersion and heating in order to evaluate the swelling and shrinking behaviour of hydrogel. The parts remained stable on the substrate and maintained the properties and the results revealed the shape retention over 97%. This work shows that VPP can be applied in the manufacturing of hydrophobic surfaces for hydrogel photopolymer deposition and curing without sacrificing critical properties.

**Keywords** Vat photopolymerization, Hydrogel, Polyethylene glycol diacrylate, Hydrophobic surfaces

## Introduction

Hydrogels have obtained a widespread interest of research and industry because of their diversified properties, such as water absorption without dissolution, biocompatibility and flexibility. Among synthetic hydrogels, PEGDA has become a focus of studies due to combination of manifold characteristics. It is a highly reactive polymeric material, synthesized from a polyethylene glycol (PEG) precursor and diacrylate (DA) crosslinker. PEGDA-based components can swell under immersion in water, and upon exposure to sufficiently high temperature, regain their initial shape. Additionally, due to the feasibility for modification of hydroxyl groups, PEGDA can be customised and processed with numerous

fabrication methods, such as spin coating, chemical vapour deposition, and electropolymerization [1, 2]. Thus, PEGDA is extensively used in humidity sensing devices in quartz tuning forks [3], tissue engineering for cells proliferation [4, 5] and controlled substance release capsules in drug delivery systems [6].

An emerging application of PEGDA-based hydrogels are thin films and coatings. They have been reported as a promising component for antibacterial, antifouling and immunoprotective layers [1, 7]. In this application, hydrogel can be designed as the protecting film or chemically altered to function as an independent agent to form a barrier for antimicrobial substances [8–11]. Example of devices in which PEGDA-based films have the potential to significantly improve the performance and life-span are dialysis media and hearing aids, which require to be equipped with filters to prevent environmental and microbial contamination [12]. The filters are difficult to clean due to small size of the mesh and therefore they are often single-use, generating waste. To overcome this issue a porous, net-shaped hydrogel membrane

\*Correspondence:

Anna Danielak  
annada@dtu.dk

<sup>1</sup> Department of Civil and Mechanical Engineering, Technical University of Denmark, Kgs. Lyngby, Denmark

<sup>2</sup> Department of Mechanical Engineering, Korea Advanced Institute of Science and Technology, Daejeon, Republic of Korea

can be attached as a supplementary physical and chemical barrier simultaneously providing a sufficient flow of the desired substances. Contaminated filter can be submerged in water to trigger the swelling and expansion of the structure. With enlarged net, the pollutants can be easily removed leaving the device clean. Finally, by applying heat, the hydrogel filter can be recovered to its initial shape and reused.

PEGDA-based hydrogels, however, have low mechanical properties and are susceptible to damage upon handling, which require the parts to be suspended or chemically bonded to a substrate. This significantly prohibits the flow of substances and lateral swelling or can lead to part damage when subjected to mechanical loads [13–15]. It can be overcome by direct fabrication of the part on the device, but such a method requires deposition of the hydrogel in a non-polymerized liquid state, which can leak through the substrate. Therefore, a liquid-repellent base is preferable. This can be achieved by applying a hydrophobic surface, which is a specially designed surface for liquid retention by means of increasing the contact angle between the liquid droplet and the substrate [16]. Such surfaces generate a great interest in applications that require controlled wettability, corrosion resistance, anti-freezing, anti-bioadhesive, liquid transportation and many others [17]. To fabricate a component where a hydrogel part is attached to a hydrophobic surface, a two-step manufacturing process needs to be adapted. In such approach, a hydrophobic surface is fabricated first and serves as a substrate for PEGDA hydrogel deposition and polymerization. Due to complexity of the surface, a suitable method, which can provide high fidelity and resolution, is required. Among available processes, vat photopolymerization additive manufacturing (abbreviated as VPP) is the most suitable method as it is characterized by a high level of customization, a wide range of available materials and high resolution allowing for production of parts at a sub-millimetre scale, which are required for fabrication of ultra-complex microstructures. It is a process that employs structured ultraviolet (UV) light to crosslink a liquid polymer and create a solid structure [18]. The parts made by VPP are built layer-by-layer, where the area exposed to irradiance is the cross section of the produced part with a defined thickness. The subsequent layers are added by moving the build plate in the vertical direction. In addition, there are two types of light excitation: focused laser beam and mask projection, which uses a high-resolution projector with either Liquid Crystal Display (LCD) or Digital Micromirror Device (DMD™). The level of photopolymerization can be controlled by optimization of main process parameters, which are layer thickness, irradiance level of the UV light and exposure time [19]. VPP

has found application in fields such as custom-fit hearing aids, dental crowns, robotics, functional surfaces and soft tooling [20, 21]. VPP techniques can be also used for processing of PEGDA hydrogels, which, when combined with photoinitiator and exposed to UV light, can undergo free radical photopolymerization, due to double-bond acrylate groups at the ends of the PEG chain [22].

This work proposes a process chain, in which mask-projection VPP technique is used for manufacturing of hydrophobic substrate for hydrogel deposition. The hydrogel is subsequently cured into a solid pattern and subjected to water immersion and heating experiment to evaluate the influence of the surface on the swelling-shrinking behaviour. This novel approach explores the feasibility of application of hydrophobic structure for facilitated hydrogel parts manufacturing and application without the loss of the properties of the hydrogel.

## Materials and methods

### Design, materials and fabrication

The proposed structure was designed as a two-component assembly made of a liquid-repellent substrate and a simple hydrogel feature located at the apex. To imitate the filtering device, both components had vertically aligned apertures and their overall dimensions were interdependent. The overview of the part is shown in Fig. 1. The substrate function was to provide a base for the liquid hydrogel deposition, photopolymerization and the swelling and shrinking procedure. For this purpose the specimens fabrication was divided into two stages. First, the base was designed as a hydrophobic surface and manufactured using mask projection VPP setup. Next, a photoreactive hydrogel was synthesised, deposited on the surface and cured used a specially designed ultra high-resolution photopolymerization setup.

### Liquid-repellent base

The base was designed following the Cassie-Baxter state, in which the hydrophobicity occurs due to

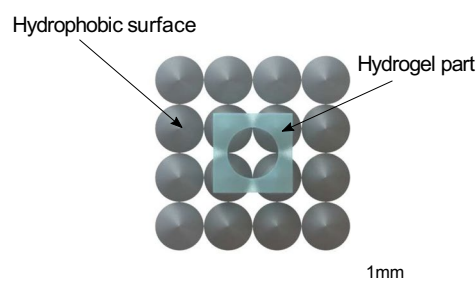


**Fig. 1** Top-view of the hydrogel part and the hydrophobic surface assembly

roughness-induced formation of air pockets between the surface and the liquid droplet [23]. Such surfaces are often made from pillar-like structures, with wider, re-entrant upper part and pointed or spiky tops for roughness enhancement [24, 25]. Cassie-Baxter model is preferable for the proposed components configuration, as it elevates the liquid above the air pockets, instead of allowing it to penetrate through the features of the surface. The surface was designed by assembling a  $4 \times 4$  array of dome-shaped features with sharp tips, then placed on the pillar to trap the air between the deposited material and the substrate. The dimensions of the features were based on several constraints, deriving from the resolution of the VPP unit, curing characteristics of the resin and surface design aspects (i.e. micro-scale and arrayed arrangement). The pillars' diameter was set to 0.6 mm, as smaller values led to delamination of layers due to pulling forces during vertical movement of the build plate. The diameter of the dome was dependent on the inclination angle of the re-entrant structure. It was selected at  $60^\circ$  relative to the horizontal plane ( $150^\circ$  from the pillar) as the previous study determined that, despite it being possible to achieve a lower angle, an overcuring typically takes place under the inclination as an effect of the staircase effect [26]. The  $90^\circ$  angle of the top of the structure was a trade-off between preferred enhanced roughness and low staircase effect. The close distance between the single re-entrant structures aimed to simulate the interconnected net structures, like in filtering devices. The final feature is depicted in Fig. 2a. The overview of the part can be seen in Fig. 2b.

The commercial Anycubic<sup>®</sup> Photon S desktop bottom-up, mask projection VPP unit was applied for the base fabrication. The system uses a 405 nm LCD projector with resolution of  $2560 \times 1440$  pixels, a pixel pitch of  $47 \mu\text{m}$  and 50 W rated power. The specimens were manufactured at 4 s of exposure time and layer thickness of  $50 \mu\text{m}$ . The post-processing included cleaning with isopropanol in an ultrasonic unit for 10 min, air-dried by a pressurised nitrogen and post-cured in a flood-light UV-light unit for 20 min. The material for the surface was a commercial FTD<sup>®</sup> SnowWhite photopolymer resin.

#### Hydrogel-based parts

PEGDA-based photopolymer resin of two molecular weights were prepared;  $M_n = 250 \text{ g/mol}$  and  $M_n = 575 \text{ g/mol}$ , further referred to as PEGDA250 and PEGDA575. The monomer was synthesized with Phenylbis (2,4,6-trimethylbenzoyl)phosphine oxide (97%) photoinitiator for radical polymerization (2wt%). An additional solution consisting of PEDGA250, photoinitiator and 1-(Phenyldiazetyl)naphthalen-2-ol (known as Sudan I, 0.7wt%) was prepared. Sudan I inhibits the UV curing rate, therefore

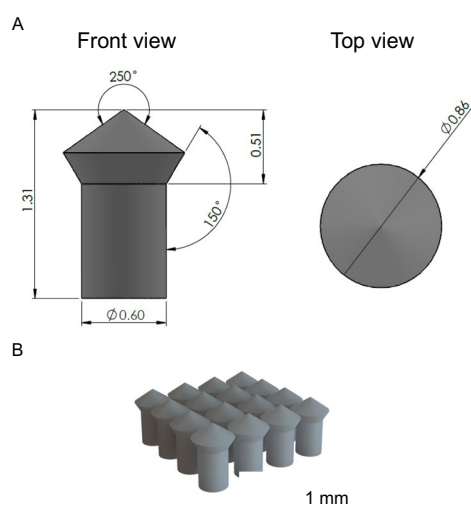


**Fig. 2** Hydrophobic base. **a** Single feature. **b** Overview of the entire part

is often used for high-resolution features. All chemicals were purchased from Merck. The solutions were mixed with magnetic stirrer at 120 rpm for 24 hrs at a room temperature.

The parts were fabricated using in-house developed high-resolution mask-projection system using 10x objective lens capable of achieving pixel size of  $1.3 \mu\text{m}$  [27]. It has a standard resolution of  $1930 \times 1080$  pixels and the maximum image size of  $3.46 \times 1.94 \text{ mm}$ . In this setup, it is possible to enlarge the building envelope by applying a lens with higher magnification, at the expense of limited optical diffraction and therefore pixel size. In this study, the 10x lens supplied a sufficient trade-off between the resolution and maximum patterning area. The mask projection is realised with a 405 nm UV-light emitting diode, a DLP LightCrafter<sup>™</sup> 6500 EVM DMD<sup>™</sup> module from Texas Instruments<sup>™</sup>, modular elements for light manipulation (lens, mirror and beam splitter) and a CCD camera. During the process the bitmap image of the part cross-section is sent to the DMD<sup>™</sup>. It is further reflected as a light pattern by activating the selective mirrors [3]. The setup is depicted in Fig. 3.

The critical step in the manufacturing phase was determination of the exposure time and level UV-light irradiance for the hydrogel resins. For this purpose, the solutions were cured independently, before the deposition on the liquid-repellent structure. To establish the acceptable UV-dose level, a plate with micro-scale hollow affiliation logos was designed, as shown in Fig. 4a. The part was cured at varied parameters and the final settings were determined when the features were obtained, as depicted in Fig. 4b. The most satisfactory

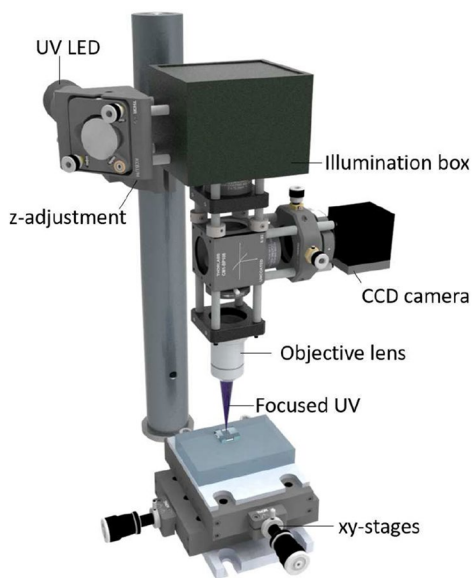


**Fig. 3** Custom-built mask projection-based VPP setup [3]

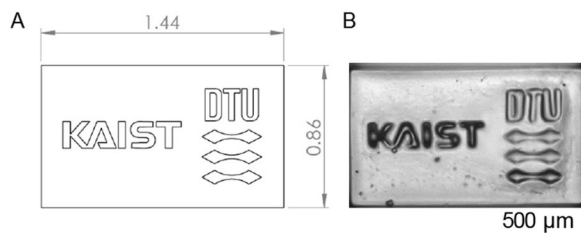


**Fig. 4** Specimen used for qualitative analysis (values in mm). **a** Part design. **b** Part made of PEGDA250

results, with the minimum feature size of approximately 10 μm, were achieved at exposure time of 0.2 s and irradiance of 38.07 mW/cm<sup>2</sup>. Minor overcuring was detected in some regions, but decrease of the UV-dose revealed lack of cross-linking. Following the curing, the parts were cleaned with ethanol.

Quantitative analysis required a simple design, which is shown in Fig. 5. The dimensions of the square corners of the specimen geometry corresponded to the centre-to-centre distance of the dome-shaped tips of the substrate. Analogically, the opening in the feature was located above the space between the pillars in the liquid-repellent base. The fabrication took place by first deposition of the liquid PEGDA resin using a syringe on the top of the hydrophobic base. Next, the pattern from the DMD™ was projected onto the material and polymerized into a tough structure. To obtain the final part, the residue hydrogel was rinsed with ethanol. Figure 6 depicts the fabrication process chain.

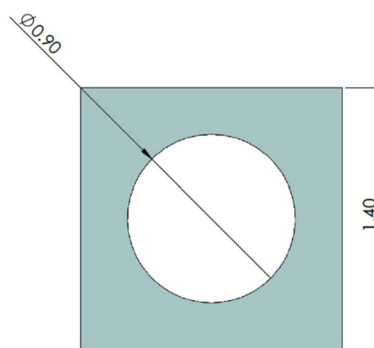


**Fig. 5** Design of the specimen used for quantitative analysis

### Hydrogel properties evaluation

#### Assessment of the hydrophobic properties of the surface

Prior to curing, the apparent contact angle (CA) between the substrate and the deposited hydrogels was measured. For the reference, the CA for water was also obtained. To additionally evaluate the efficiency of the substrate, the results were compared to CA of PEGDA-based resins deposited on a flat substrate made from the same commercial FTD® resin.

#### Dimensional stability of the parts

To evaluate the stability of the hydrogel parts with respect to the design, the diameter of the inner hole of the hydrogel feature was measured immediately after cleaning with ethanol and after 24 h. The inspection of the movement or delamination of the part was performed using microscopic pictures.

#### Swelling and shrinking properties of the hydrogel parts

The ability of the specimen to demonstrate intrinsic hydrogel behaviour - swelling and shrinking - was investigated through immersion in water followed by exposure to heat at 60 °C. Both procedures had holding time of one minute and were followed by the inner hole diameter measurement.

## Results and discussion

### Apparent contact angle

Figure 7a shows the obtained CA values. The data indicates the native hydrophilic properties of the material at the level of 65° [28], 27° and 44.5° for water, PEGDA250 and PEGDA575 respectively. From the right panel of the plot it can be seen that application of the proposed surface significantly increased the liquid repellency. The obtained CA were 112.5 ± 1.4° for water, 101.2 ± 3.7° for PEGDA250 and 99 ± 2° for PEGDA575. Figures 7b and c show the deposited PEGDA575 hydrogel on flat and

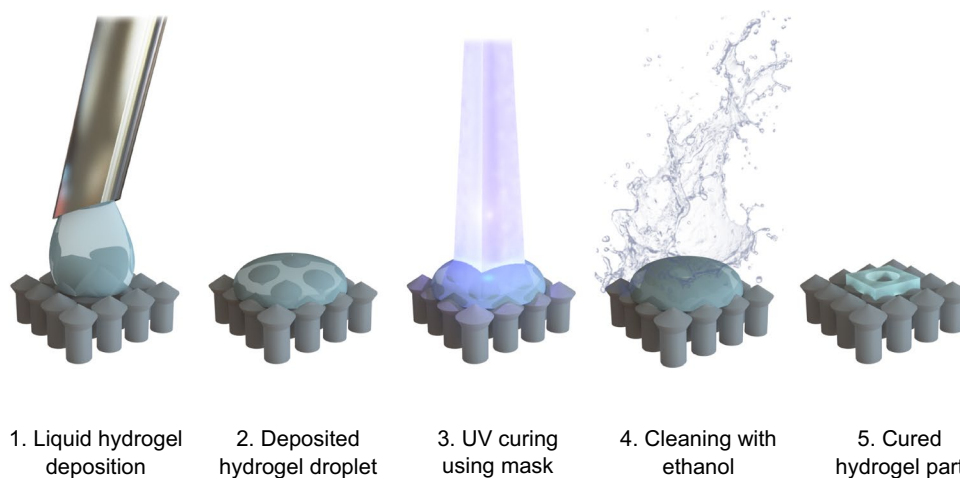


**Fig. 6** Deposition and fabrication process chain. 1,2 PEGDA hydrogel droplet deposition with a syringe. 3 A pattern curing using a UV mask. 4 Residue hydrogel rinse with ethanol. 5 Final part

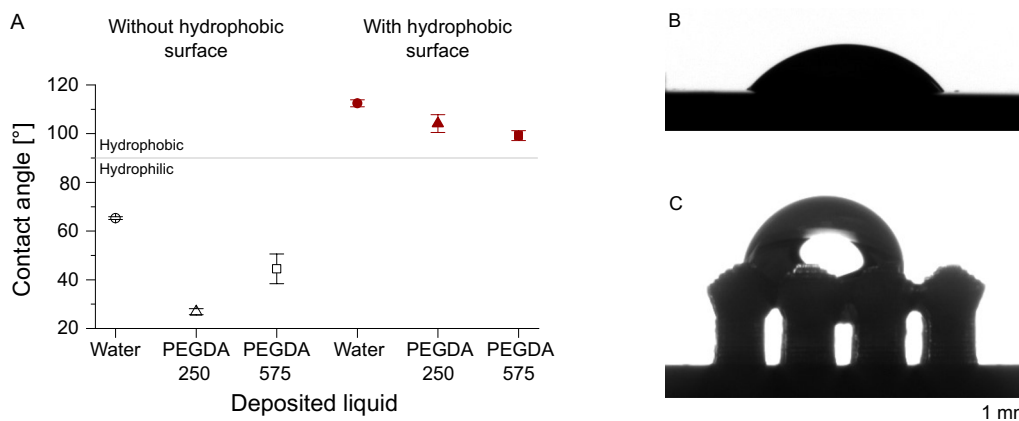


**Fig. 7** Water, PEGDA250 and PEGDA575 interaction with the substrates. **a** Static contact angle for the liquids without and with applied hydrophobic surface. **b** and **c** PEGDA575 deposited on a flat and structured substrates respectively

hydrophobic substrates and the difference in the liquid spread across the surface. Deposition of the last solution, PEGDA250+Sudan I, was not achievable as the material immediately sank inside the pillar structure due to its low surface tensions properties [29]. Therefore, it was not considered in the further study.

**Dimensional stability of the parts**

Figure 8 shows the microscope picture of the hydrogel feature after curing. Fabrication of the parts was successful for solutions with both molecular weights. A substantial amount of unpolymerized hydrogel inside the hole and on the outer space around the part can be seen in Fig. 8a. The ethanol rinse removed the remaining photopolymer, resulting in clean structure which can be seen in Fig. 8b. Upon cleaning, the part retained

fixed, indicating the efficiency of the net-like structure of the pillars assembly, which in effect supplied sufficient adhesion between the cured hydrogel and the substrate. Moreover, the empty space between the pillar features facilitated the cleaning process. The cleaning of the part is critical, as the remaining material can lead to clogging of the hole in the hydrogel feature and as an effect, distort the geometry and decrease the material properties.

Figure 9 and Table 1 show the resulting difference between the hole diameter in the hydrogel feature measured immediately after ethanol rinse and after 24 h. The initial diameter of PEGDA250 was larger in comparison to PEGDA575, which is attributed to higher number of the C=C bonds in the unpolymerized state of PEG-based hydrogels with lower molecular weight [30, 31]. As a result, in the initial stage of photopolymerization, the

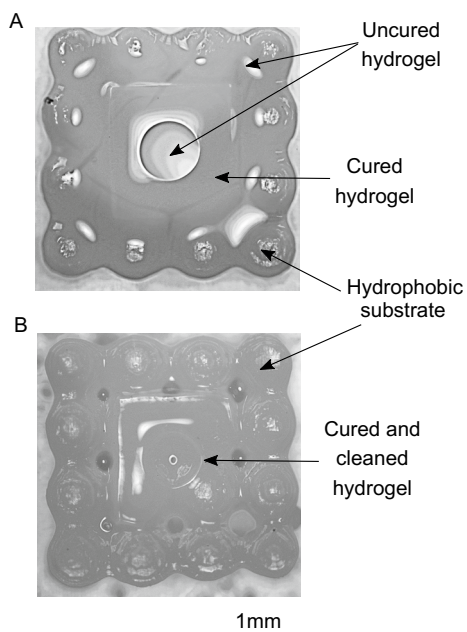


**Fig. 8** Microscopic picture of a cured feature made of PEGDA250. **a** Part before ethanol rinse. **b** Part after ethanol rinse

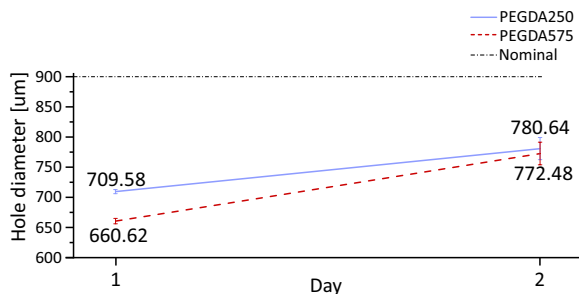


**Fig. 9** Inner hole diameter obtained directly after fabrication and after 24 h

bonds engage at a slower rate, preventing local overcuring, in this case inside the hole.

For both materials the holes experienced expansion over 24 h likely owing to the water uptake from ethanol and gradual swelling. Compared to the initial design, a decrease in the diameter was observed at a level of 119.36 μm for PEGDA250 and 127.52 μm for PEGDA575. This is due to a narrow process window resulting from very

**Table 1** Sample table title

Material	Difference	Shrinkage	Unit
PEGDA250	71.1	10	μm
PEGDA575	111.9	16.9	%

This is where the description of the table should go

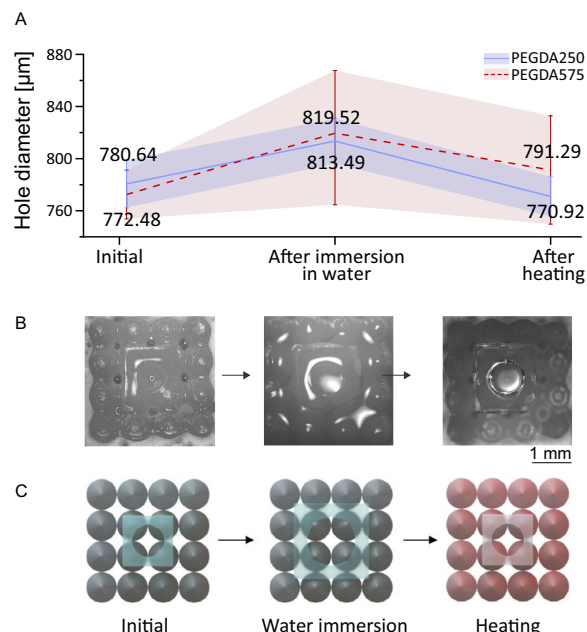


**Fig. 10** Resulting hole diameter obtained during water immersion and after heating. **a** Comparison of average values for both materials. **b** Microscopic pictures of the procedure. **c** Visualisation of the shape change of the hydrogel part

**Table 2** Diameter difference and shrinkage ratio of the holes for two different PEGDA molecular weights, experienced over 24 h

Material	Swelling	Shrinkage	Shape retention	Unit
PEGDA250	32.9	42.6	-9.7	μm
	104.2	5.2	101.3	%
PEGDA575	47.0	28.2	18.8	μm
	106.1	3.3	97.6	%

high sensitivity of hydrogel to a shift of the UV-light dose. As observed during qualitative analysis, combination of lower exposure time or irradiance resulted in complete lack of crosslinking, therefore the parameters were increased, causing overcuring inside the holes. PEGDA250 exhibited higher shape retention by 6.92%, thanks to increased crosslinking density and therefore higher structural stability [32].

**Swelling and shape retention**

The assessment of the dimensional change of the parts under water immersion and heating revealed the capability of the hydrogel to achieve the swelling-shrinking behaviour in the lateral direction while remaining in their initial position relative to the centre of the substrate. A rapid change in the diameter was recorded within

**Table 3** Diameter difference and shrinkage ratio deviations of the holes for two different PEGDA molecular weights

Material	St Dev Swelling	Value Shrinkage	Unit
PEGDA250	17.39	15.23	$\mu\text{m}$
PEGDA575	54.90	41.54	$\mu\text{m}$

10 s from exposure to water as well as heating, and it is depicted in Fig. 10a together with the standard deviations. Figure 10b shows microscopic pictures of the parts during the experiment. Table 2 shows the obtained swelling, shrinkage and shape retention ratio. Higher swelling was observed for PEGDA575, a phenomenon already reported in other studies [22, 33, 34]. As in the case of initial swelling after ethanol cleaning, this is associated with lower crosslinking density of PEGDA hydrogels with higher molecular weight, causing higher mesh size. This in effect, increases the swelling ratio due to enhanced water uptake [31, 35].

Following heating, the hole diameter of the parts made of PEGDA250 had higher shape retention. Furthermore, the dimensional change was significantly more homogeneous among the specimens, compared to PEGDA575, which exhibited high deviations, as seen in Fig. 10a and in Table 3. This is associated with lower stability of the polymer due to lower crosslinking density leading to non-uniformity of swelling and shrinking of the PEGDA575 parts [34]. As a results, large dimensional distortions took place.

The lateral shape change of the parts took place in a manner visualised in Fig. 10c. Despite the roughness of the liquid repellent substrate no mechanical damage was observed, but at the same time the two components remain concentric. This indicates limited adhesion between PEGDA and the surface, which a beneficial property for applications where hydrogel serves as an exchangeable filter.

## Conclusion

In this research, a novel approach for fabrication of PEGDA hydrogel parts on a porous substrate was developed and tested. The substrate was designed as a hydrophobic surface with a roughness-inducing features to provide a stable base for deposition and processing of hydrogel. Mask-projection vat photopolymerization additive manufacturing was chosen as a fabrication method for both surface and hydrogel parts. The net structure of the hydrophobic surface significantly facilitated the cleaning process, as the residual uncured

hydrogel could efficiently exit through the voids upon rinsing with a cleaning solvent.

The parts were further subjected to water immersion and heating in order to trigger the swelling and shirking properties. PEGDA575 experienced higher expansion rate upon water immersion, whereas PEGDA250 resulted in better shape recovery during heating. Moreover, PEGDA250 showed much higher stability in both stages of the test. The discrepancy is associated with a variation of the mesh size for hydrogels with different molecular weights.

The presented work demonstrates that the hydrophobic surface can effectively facilitate the deposition of liquid hydrogel resins for subsequent photopolymerization, and swelling and shrinking process. Throughout the experiment, no adhesive agent was required to prevent the lateral movement of the hydrogel parts without the mechanical damage, thanks to the moderate roughness of the single units of the substrate. The surface prevented delamination of the hydrogel without inhibiting the shape change, which is a common issue in the case of chemical adhesives.

To assess the full applicability of the proposed solution, a scalability study of the process chain can bring benefits for potential real-life devices. The performed experiments and obtained results can serve as a prototype and open a possibility of multi-material manufacturing for other advanced applications that require the use of hydrogels, where the reverse change in geometry is desired.

## Abbreviations

CA	Contact angle
CCD	Charge-coupled device
LCD	Liquid crystal display
DMD <sup>TM</sup>	Digital micromirror device
PDMS	Polydimethylsiloxane
PEGDA	Polyethylene glycol diacrylate
UV	Ultraviolet
VPP	Vat photopolymerization

## Acknowledgements

Not applicable.

## Author contributions

Experiment design and conceptualization: AD and JK. Machine design: JK and JL. Methodology and data analysis: AD and JK. Supervision: JL, AI and DBP. Writing and editing of the manuscript: AD, JK, AI, DBP and JL. All authors read and approved the final manuscript.

## Funding

This work was supported by Otto Mønsted's Foundation Grant 19–11-1009 and the National Research Foundation of Korea (NRF) funded by the Korea government (Ministry of Science and ICT) (NRF- 2020R1A2C3004885 and NRF- 2020R1A4A2002728).

## Availability of data and materials

All data generated or analyzed during this study are included in this published article.

## Declarations

### Ethics approval and consent to participate

Not applicable.

### Consent for publication

Authors consent the SpringerOpen license agreement to publish the article.

### Competing interests

The authors declare that they have no competing interests.

Received: 6 April 2023 Accepted: 25 May 2023

Published online: 07 June 2023

## References

- Tokarev I, Minko S (2009) Stimuli-responsive hydrogel thin films. *Soft Matter* 5(3):511–524
- Uribe-Lam E, Treviño-Quintanilla CD, Cuan-Urquiza E, Olvera-Silva O (2021) Use of additive manufacturing for the fabrication of cellular and lattice materials: a review. *Mater Manuf Proc* 36(3):257–280
- Ko J, Yoon Y, Lee J (2018) Quartz tuning forks with hydrogel patterned by dynamic mask lithography for humidity sensing. *Sens Actuators B Chem* 273:821–825. <https://doi.org/10.1016/j.snb.2018.06.099>
- Chartrain NA, Williams CB, Whittington AR (2018) A review on fabricating tissue scaffolds using vat photopolymerization. *Acta Biomater* 74:90–111. <https://doi.org/10.1016/j.actbio.2018.05.010>
- Chua CK, Yeong WY (2015) Material for bioprinting. In: *Bioprinting*, pp. 117–163. World Scientific, New York
- Santos ARC, Almeida HA, Bártolo PJ (2013) Additive manufacturing techniques for scaffold-based cartilage tissue engineering: a review on various additive manufacturing technologies in generating scaffolds for cartilage tissue engineering. *Virtual Phys Prototyp* 8(3):175–186. <https://doi.org/10.1080/17452759.2013.838825>
- González-Henríquez CM, Sarabia-Vallejos MA, Rodríguez-Hernández J (2017) Advances in the fabrication of antimicrobial hydrogels for biomedical applications. *Materials* 10(3):1–24. <https://doi.org/10.3390/ma10030232>
- Don TM, Chen CC, Lee CK, Cheng WY, Cheng LP (2005) Preparation and antibacterial test of chitosan/PAA/PEGDA bi-layer composite membranes. *J Biomater Sci Polym Ed* 16(12):1503–1519. <https://doi.org/10.1163/156856205774576718>
- Huang L, Zhu Z, Wu D, Gan W, Zhu S, Li W, Tian J, Li L, Zhou C, Lu L (2019) Antibacterial poly(ethylene glycol) diacrylate/chitosan hydrogels enhance mechanical adhesiveness and promote skin regeneration. *Carbohydr Polym* 225(May):1–12. <https://doi.org/10.1016/j.carbpol.2019.115110>
- Lilly JL, Romero G, Xu W, Shin HY, Berron BJ (2015) Characterization of molecular transport in ultrathin hydrogel coatings for cellular immunoprotection. *Biomacromolecules* 16(2):541–549. <https://doi.org/10.1021/bm501594x>
- Liu SQ, Yang C, Huang Y, Ding X, Li Y, Fan WM, Hedrick JL, Yang YY (2012) Antimicrobial and antifouling hydrogels formed in situ from polycarbonate and poly(ethylene glycol) via Michael addition. *Adv Mater* 24(48):6484–6489. <https://doi.org/10.1002/adma.201202225>
- Surace R, Bellantone V, Trotta G, Basile V, Modica F, Fassi I (2016) Design and fabrication of a polymeric microfilter for medical applications. *J Micro Nanomanuf* 4(1):1–5. <https://doi.org/10.1115/1.4032035>
- Almany L, Seliktar D (2005) Biosynthetic hydrogel scaffolds made from fibrinogen and polyethylene glycol for 3D cell cultures. *Biomaterials* 26(15):2467–2477
- Senior JJ, Cooke ME, Grover LM, Smith AM (2019) Fabrication of complex hydrogel structures using suspended layer additive manufacturing (SLAM). *Adv Funct Mater* 29(49):1–10. <https://doi.org/10.1002/adfm.201904845>
- Vedadghavami A, Minooei F, Mohammadi MH, Khetani S, Rezaei Kolahchi A, Mashayekhan S, Sanati-Nezhad A (2017) Manufacturing of hydrogel biomaterials with controlled mechanical properties for tissue engineering applications. *Acta Biomater* 62(July):42–63. <https://doi.org/10.1016/j.actbio.2017.07.028>
- Jeevahan J, Chandrasekaran M, Britto Joseph G, Durairaj RB, Mageshwaran G (2018) Superhydrophobic surfaces: a review on fundamentals, applications, and challenges. *J Coat Technol Res* 15(2):231–250. <https://doi.org/10.1007/s11998-017-0011-x>
- Matin A, Merah N, Ibrahim A (2016) Superhydrophobic and self-cleaning surfaces prepared from a commercial silane using a single-step drop-coating method. *Prog Org Coat* 99:322–329. <https://doi.org/10.1016/j.porgcoat.2016.06.007>
- Ligon SC, Liska R, Stampfl J, Gurr M, Mülhaupt R (2017) Polymers for 3D printing and customized additive manufacturing. *Chem Rev* 117(15):10212–10290. <https://doi.org/10.1021/acs.chemrev.7b00074>
- Gibson I, Rosen D, Stucker B (2015) Vat photopolymerization processes. *Add Manuf Technol*. [https://doi.org/10.1007/978-1-4939-2113-3\\_4](https://doi.org/10.1007/978-1-4939-2113-3_4)
- Stansbury JW, Idacavage MJ (2016) 3d printing with polymers: challenges among expanding options and opportunities. *Dent Mater J* 32(1):54–64. <https://doi.org/10.1016/j.dental.2015.09.018>
- Saxena P, Bissacco G, Meinert KE, Danielak AH, Ribó MM, Pedersen DB (2020) Soft tooling process chain for the manufacturing of micro-functional features on molds used for molding of paper bottles. *J Manuf Proc* 54:129–137. <https://doi.org/10.1016/j.jmapro.2020.03.008>
- McAvoy K, Jones D, Thakur RRS (2018) Synthesis and characterisation of photocrosslinked poly(ethylene glycol) diacrylate implants for sustained ocular drug delivery. *Pharm Res* 35(2):1–17. <https://doi.org/10.1007/s11095-017-2298-9>
- Chen L, Guo Z, Liu W (2017) Outmatching superhydrophobicity: bio-inspired re-entrant curvature for mighty superamphiphobicity in air. *J Mater Chem A Mater* 5(28):14480–14507. <https://doi.org/10.1039/c7ta03248j>
- Jafari R, Cloutier C, Allahdini A, Momen G (2019) Recent progress and challenges with 3D printing of patterned hydrophobic and superhydrophobic surfaces. *Int J Adv Manuf Technol* 103(1–4):1225–1238. <https://doi.org/10.1007/s00170-019-03630-4>
- Davoudinejad A, Ribó MM, Pedersen DB, Islam A, Tosello G (2018) Direct fabrication of bio-inspired gecko-like geometries with vat polymerization additive manufacturing method. *J Micromech Microeng* 28(8):1–10. <https://doi.org/10.1088/1361-6439/aabf17>
- Danielak AH, Ribó MM, Pedersen DB, Islam A (2018) Characterisation of the influence of the colour in resin for micro parts production by photopolymerisation based additive manufacturing system. In: *Proceedings - 2018 ASPE and Euspen Summer Topical Meeting: Advancing Precision in Additive Manufacturing*
- Yoon Y, Chae I, Thundat T, Lee J (2019) Hydrogel microelectromechanical system (MEMS) resonators: beyond cost-effective sensing platform. *Adv Mater Technol* 4(3):1–11. <https://doi.org/10.1002/admt.201800597>
- Danielak A (2021) Design, optimization and production of smart surfaces by additive manufacturing for medical applications. PhD thesis, Technical University of Denmark, Mechanical Engineering
- Zhang K, Xie R, Fang K, Chen W, Shi Z, Ren Y (2019) Effects of reactive dye structures on surface tensions and viscosities of dye solutions. *J Mol Liq* 287:110932. <https://doi.org/10.1016/j.molliq.2019.110932>
- Sung J, Lee DG, Lee S, Park J, Jung HW (2020) Crosslinking dynamics and gelation characteristics of photo- and thermally polymerized poly(ethylene glycol) Hydrogels. *Materials* 13(15):1–12. <https://doi.org/10.3390/ma13153277>
- Weber LM, Lopez CG, Anseth KS (2009) The effects of PEG hydrogel crosslinking density on protein diffusion and encapsulated islet survival and function. *J Biomed Mater Res* 90:720–729. <https://doi.org/10.1002/jbma.a.32134>
- Lu S, Anseth KS (2000) Release behavior of high molecular weight solutes from poly(ethylene glycol)-based degradable networks. *Macromolecules* 33(7):2509–2515. <https://doi.org/10.1021/ma9915024>
- Peppas NA, Keys KB, Torres-Lugo M, Lowman AM (1999) Poly(ethylene glycol)-containing hydrogels in drug delivery. *J Control Rel* 62(1–2):81–87. [https://doi.org/10.1016/S0168-3659\(99\)00027-9](https://doi.org/10.1016/S0168-3659(99)00027-9)
- Raj Singh TR, McCarron PA, Woolfson AD, Donnelly RF (2009) Investigation of swelling and network parameters of poly(ethylene glycol)-crosslinked poly(methyl vinyl ether-co-maleic acid) hydrogels. *Eur Polym J* 45(4):1239–1249. <https://doi.org/10.1016/j.eurpolymj.2008.12.019>

35. Mellott M, Searcy K, Pishko MV (2001) Release of protein from a highly cross-linked hydrogel of poly(ethylene glycol) diacrylate fabricated by UV polymerization. *Biomaterials* 22(9):929–941. [https://doi.org/10.1016/S0142-9612\(00\)00258-1](https://doi.org/10.1016/S0142-9612(00)00258-1)

### **Publisher's Note**

Springer Nature remains neutral with regard to jurisdictional claims in published maps and institutional affiliations.

**Submit your manuscript to a SpringerOpen<sup>®</sup> journal and benefit from:**

- ▶ Convenient online submission
- ▶ Rigorous peer review
- ▶ Open access: articles freely available online
- ▶ High visibility within the field
- ▶ Retaining the copyright to your article

---

Submit your next manuscript at ▶ [springeropen.com](https://www.springeropen.com)

---